

RESIDUAL GAS DISTRIBUTION IN VUGGY CARBONATE BY USE OF X-RAY CT, NMR AND CRYO-ESEM

Ann Lisbeth Bye, Lars Rennan, Hege C. Widerøe, Tony Boassen and Jon K. Ringen,
StatoilHydro ASA, Norway

*This paper was prepared for presentation at the International Symposium of the
Society of Core Analysts held in Abu Dhabi, UAE 29 October-2 November, 2008*

ABSTRACT

Vuggy carbonate samples from an outcrop formation have been studied using in-situ monitoring techniques; both porosity and saturation distribution.

- NMR to quantify distribution between matrix porosity and vugs on the sample scale
- X-ray CT for local saturation distribution in matrix vs. vugs on a mm-scale
- Cryo-ESEM to describe vugs and saturation distribution on a micro scale

The samples studied have a porosity of 24% and vugs are in the range of 0,2-10 mm. The NMR measurements indicate that the vugs contribute to 55% of the porosity. CT studies show that most vugs are not in direct communication with each other. Swi from centrifuge drainage is only slightly higher in the tighter matrix than in the vuggy part of the pore system. Sgr after waterflood is significantly lower in the vuggy parts than in the matrix. Cryo-ESEM at Swi revealed vugs saturated with brine, as well as vugs almost fully drained. Similar for Sgr; some vugs were efficiently flooded and some showed high residual saturation.

INTRODUCTION

Vuggy carbonate formations provide extra challenges with respect to static characteristics and dynamic fluid behaviour. The permeability and hydrocarbon recovery will be affected by the degree of connectivity between vugs; either through the matrix pore network, via fractures or direct contact. In addition, waterflood recovery is likely to be dependent on the wettability distribution. Methods of in-situ porosity distribution and saturation monitoring would be valuable for studying vuggy core material behaviour. The methods would have to distinguish vugs from matrix and this demands image resolution and sample stability. Several experimental studies have been undertaken using in-situ techniques to describe vug/matrix pore systems. NMR and to some extent CT has been used to study local gas or oil recovery (Hijadat *et al.*, 2002; Olivier *et al.*, 2004; Egerman, *et al.*, 2004; Moctezuma-Berthier and Fleury, 1999). In this work we try to make maximum use of a “standard” CT to quantify the distribution of residual saturations in vugs versus matrix in a completely water wet system.

PROCEDURE AND RESULTS

Core Material and Fluids

The samples used in this study are vuggy core material obtained from CIPR (Centre for Integrated Petroleum Research, University of Bergen, Norway) (Vik *et al.*, 2007), originating from the Prebetic subzone of the Betic range (Spain). The vug sizes are in the

range of 0.2-10 mm, porosity was measured to be 24 % and brine permeability 12 D. Pc(air/water) drainage by centrifuge is shown in Figure 1. The porosity distribution from CT for one slice is shown in Figure 2. The brine used in CT experiments was 3% NaCl + 4% NaI and air. Brine with NaI gives a good contrast on CT images. 3% NaCl was used in the NMR and cryo-ESEM, in addition to refined lab oil.

NMR Porosity And Pore Size Distribution

NMR measurements were performed in order to estimate the fraction of the vuggy pore volume in the carbonate plug using a Maran DRX NMR spectrometer operating at 12.8 MHz. The spectrometer is equipped with a 225 Gauss/cm magnetic field gradient, enabling diffusion-weighted measurements. The cleaned, dry core plug was saturated with brine (vac + pressure). Combined T_1 , T_2 , and diffusion measurements at short observation times were performed in order to determine a pore size distribution (μm) and to estimate the vuggy porosity. Two different processing tools for the T_1 - T_2 data were used; ANAHES, (Ukkelberg *et al.*, 2007) and an algorithm producing 2D contour plots (Godefroy *et al.*, 2003). NMR T_2 values were converted to pore sizes by the average surface-to-volume ratio (S/V) found in the diffusion measurement (Sørland *et al.*, 2007). 2D T_1 - T_2 clearly resolved at least 3 major peaks, see Figure 3. The largest pores gave rise to a signal at a T_2 of about 2 sec, and a T_2 cut off for vugs was chosen at 1 sec. The cut off corresponds to a V/S of about 0.8 mm, with vugs representing about 55 % of the porosity.

X-ray CT Residual Gas Flooding Experiment

The CT scanner used is a fourth generation medical type scanner Picker PQ-6000 with the maximum spatial resolution of 350 μm . The slice thickness is 2 mm and an image size of 60 mm gives a pixel resolution of 0.12 x 0.12 mm. Two 1,5 inch diameter plugs were solvent cleaned and saturated by brine (vac + pressure). $S_{wi}(g)$ was established by centrifuging w/air. The plugs were mounted in a core holder as a composite core and water flooded at 5 ml/h to residual gas saturation, $S_{gr}(w)$. The brine was saturated w/air at the pore pressure used, 10 bars. CT scans were performed at $S_{wi}(g)$ and every minute as the core was flooded towards S_{gr} . When gas production ceased, the core was water flooded at high rates to observe any mobilization of the trapped gas; 30, 120 and 600 ml/h. A CT scan at final S_{gr} was performed. Figure 4 shows CT images at different stages in the experiment. CT scans at $S_w=1$ and dry core were performed afterwards as reference scans and to determine local porosity. Figure 5 shows all CT pixel values as S_{gr} vs porosity. CT scanning for saturation distribution was performed with the sample fixed in one position to minimize data noise and all images are from one selected CT slice in the core plug.

Fluid Distribution By cryo-ESEM

The electron microscope used is a FEI Quanta 400 equipped with a ThermoNoran Vantage EDS system. The ESEM is operated in low vacuum mode with nitrogen inlet gas. The accelerating voltage was 15kV and the working distance 10mm. One cleaned core plug was drained to S_{wi} with air in centrifuge, then the air was replaced by refined lab oil. The plug then spontaneously imbibed water before spinning in centrifuge for forced imbibition to S_{orw} . Finally a forced drainage back to S_{wi} was performed. At all stages small pieces were broken off the plug for cryo-ESEM investigations.

DISCUSSION AND CONCLUSIONS

The NMR surface-to-volume ratio S/V is uncertain, possibly due to convection in large voids, observed as diffusion coefficients somewhat higher than for bulk water. This should be further addressed, and a convection compensated measurement might be necessary. The CT porosity histogram in Figure 4 does not show any bimodal porosity distribution, but a long tail of porosities up to 86 %. This is a result of CT values in vugs being affected by signals from the matrix, and matrix being affected by vugs. Combining the histogram with the NMR cut off value at 55% for porosity from vugs, we get a corresponding CT porosity cut off value of 25%. If a pixel has porosity $> 25\%$ we have vugs and $< 25\%$ we have matrix and normal pores. This gives us a threshold for interpreting the CT data, but does not resolve the vug porosity from CT directly. The porosity distribution image for one slice in Figure 4 shows vugs as red and pink areas with a porosity gradient towards the matrix boundary as blue.

Figure 5 shows the correlation of S_{gr} vs. porosity for all pixels. Also presented is the distribution of vugs and water distribution for one slice, indicating low S_w in vuggy areas. To investigate further the S_{wi} and S_{gr} saturations for vugs versus matrix, the CT pixel porosity was grouped into classes of 10 porosity units. The two lowest porosity classes are interpreted to represent only matrix porosity, while the three highest classes represent vuggy porosity. The classes in the middle represent a mix of matrix and vugs. The corresponding water saturation at S_{wi} and S_{gr} are plotted in Figure 6. The figure shows a fairly uniform S_{wi} distribution, with slightly S_{wi} in the matrix as could be expected due to capillary forces. After low rate water flooding to S_{gr} , the high porosity classes have lower water saturation (higher S_{gr}) compared to the lower porosity classes. Increasing the flow rate produced more gas from the core. The porosity classes representing vugs show a significant increase in S_w (lower S_{gr}). Also, the water saturation in the matrix pore classes actually decreased, although very slightly. Our interpretation is that the increased viscous force made the gas trapped in the vugs overcome the capillary threshold and was produced out the core via the matrix and other vugs.

For the Cryo-ESEM, the large pores and vugs give an uncertainty to the measurements. Spontaneous imbibition with water shows that water overall is in contact with the surface of pores and vugs, but oil are also found to be in contact some places as shown in Figure 7. After forced imbibition with water to S_{orw} the oil is often located in small vugs and pores often surrounded by a film of water. When the sample is drained back to S_{wi} again, the water is located in matrix porosity and in some small vugs. From this we conclude that the material is water wet to mixed wet.

These observations confirm that vugs play an important role in recovery by waterflood. Vugs can remain un-flooded or have high residual saturation due to water flowing in the matrix. This is applicable to a water wet system as studied. We also show that CT imaging together with NMR and cryo-ESEM techniques can give a good visualization of fluid distribution and movement in a vuggy system.

ACKNOWLEDGEMENT

We are grateful to Prof. Paul Callaghan, University of Wellington, New Zealand, for the supply of the 2D ILT software, to Dr. Åsmund Ukkelberg, University of Oslo, Norway, for the ANAHES transform, and to Dr. Geir Humborstad Sørland, AnTek, Norway, for the recording of the NMR data. We would also thank CIPR, University in Bergen for the assistance and supply of core material.

REFERENCES

1. Boassen T, Kowalewski E, Hemmingsen PV. "Cryo SEM studies of emulsions and fluid distribution at pore scale", SCA2006-43, presented at SCA Symposium in Trondheim, Norway, 2006.
2. Egerman P, Laroche C, Delamaide E, Bourbieux B. "Experimental and Numerical Study of Water-Gas imbibition Phenomena in Vuggy Carbonates". SPE 89421, 2004.
3. Hidajat I, Mohanty KK, Flaum M, Hirasaki G. "Study of Vuggy Carbonates using X-Ray CT Scanner and NMR" SPE 77396, 2002.
4. Moctezuma-Berthier A, Fleury M. "Permeability Mapping on Vuggy Core Sample Using Tracer Experiments and StreamLine Simulations". SCA-9919 presented at Society of Core Analysts International Symposium, 1999.
5. Olivier P, Cantegrel L, Laveissiere J, Guillonneau N. "Multiphase Flow behaviour in Vugular Carbonates using X-Ray CT. SCA2004-13, 2004
6. Sørland GH, Djurhuus K, Widerøe HC, Lien JR, Skauge A. "Absolute pore size distribution from NMR". *Diffusion Fundamentals* (2007) **5**: 4.1-4.15
7. Ukkelberg Å, Sørland GH, Hansen EW, Widerøe HC. "ANAHES, a New Second Order Inverse Laplace Transform Algorithm, with NMR applications", Poster presentation at Diffusion Fundamentals II, Basic Principles of Theory, Experiment and Application, L'Aquila, Italy, August 26th - 29th, 2007.
8. Vik B, Djurhus K, Spildo K, Skauge A. "Characterisation of Vuggy Carbonates". SPE 111434, 2007.

FIGURES AND TABLES

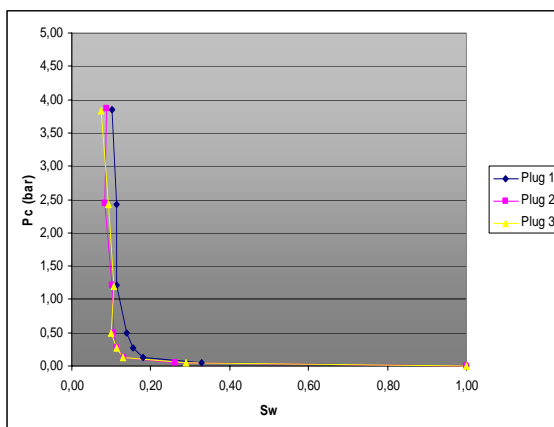


Figure 1. Gas/water capillary pressure from primary drainage in centrifuge.
3 outcrop plugs used in the study.

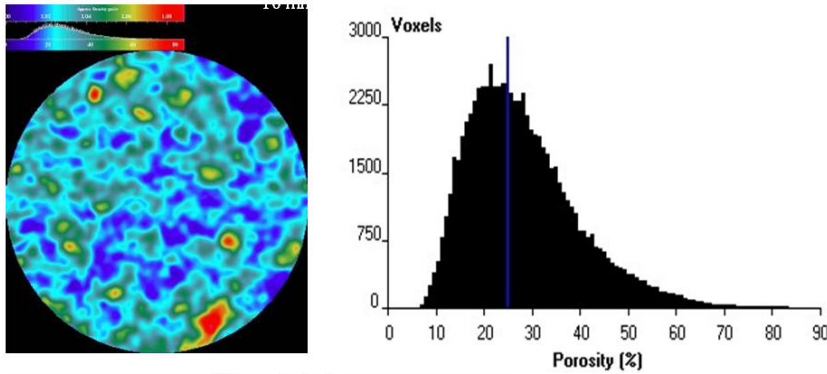


Figure 2.
Porosity distribution from CT scans. Porosity image to the left (blue is low porosity, red is high). Histogram of porosity on the right.

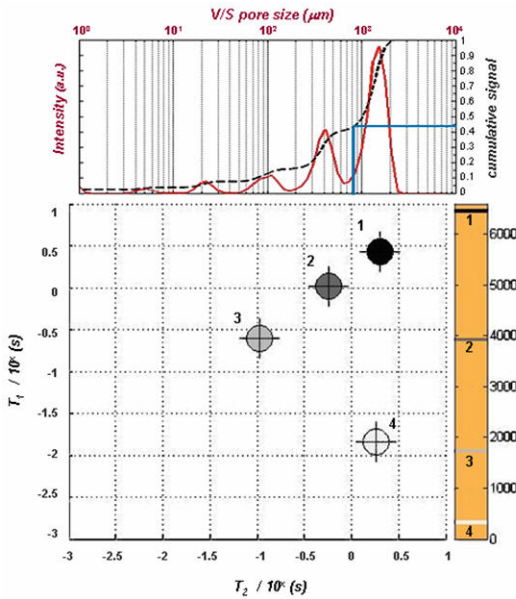


Figure 3: NMR
2D T_1 - T_2 recording (a) processed with ANAHNESS, showing the main T_1 - T_2 components in a 2D plot and (b) processed initially as a contour plot which was then projected onto the T_2 -axis and converted to pore size, giving a 1D pore size distribution (red solid line). Its cumulative porosity is included (dashed line), showing the cutoff for the vuggy porosity (blue marks). The intensity of the respective T_1 - T_2 components in (a) were (1) 6460, (2) 2945, (3) 1766, and (4) 374.

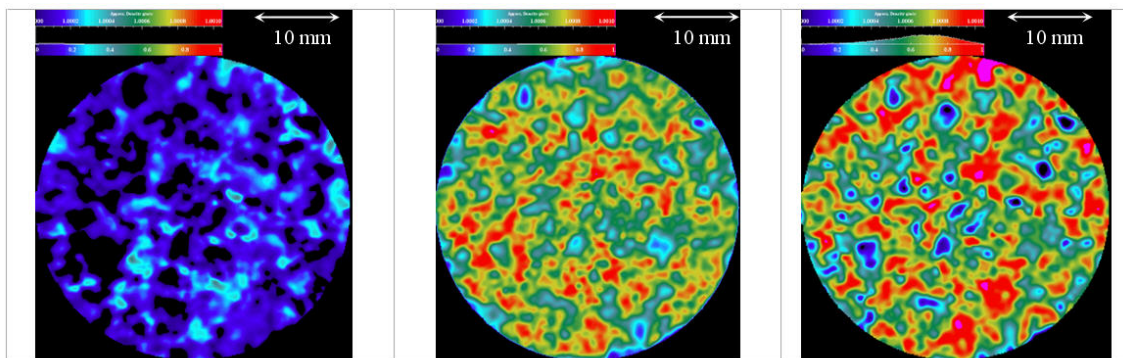


Figure 4. X-ray CT saturation distribution during waterflooding. Water saturation at S_{wi} (left), after low rate water flooding (middle) and high rate flooding (right). Blue is low water saturation and red/pink high water saturation.

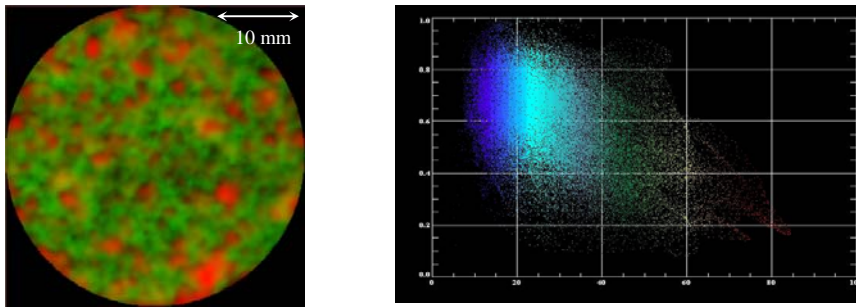


Figure 5. Sgr after low rate waterflood vs Porosity from CT. Left image: Combined image with high porosity = red and high water saturation = green. Right image: Cross plot of porosity (x-axis) versus Sw (y-axis) after low rate flooding to the right, all CT pixels.

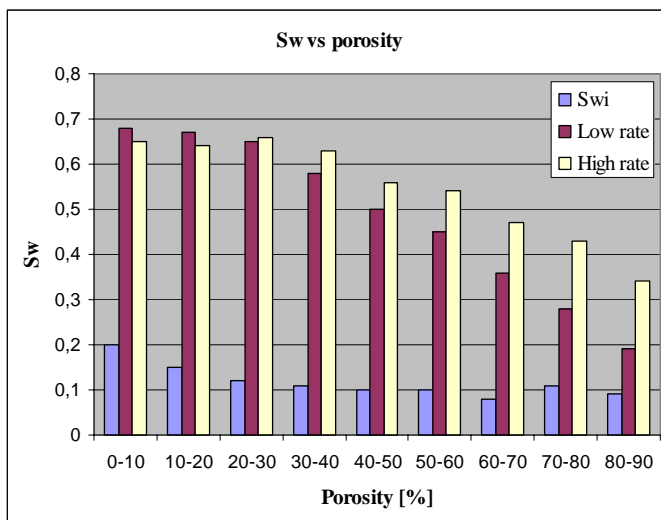


Figure 6. X-ray CT saturation distribution before/after waterflooding.

CT-pixels as porosity classes (x-axis). Swi distribution (blue). Sw after low rate waterflood to Sgr (red). Sw after high rate waterflood (yellow)

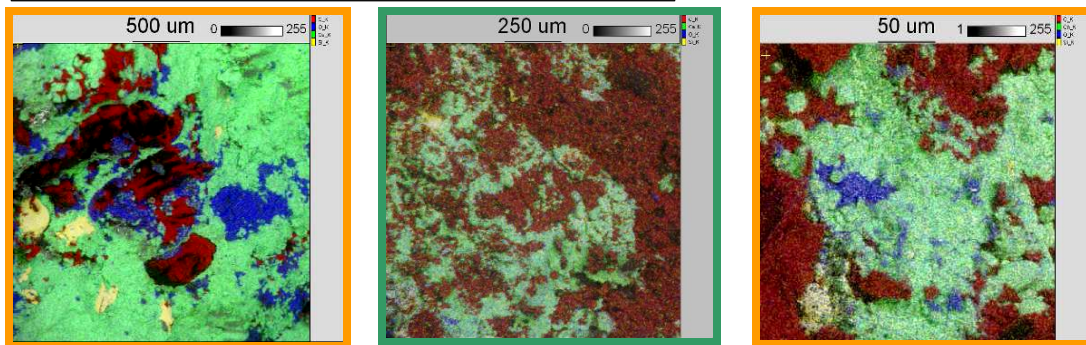


Figure 7. Cryo-ESEM. The image to the left shows example of distribution of spontaneously imbibed sample after Swi (o/w). Green colour is matrix w/pores. Red colour is oil, here mainly in large vugs. Blue colour is water, mainly in small pores, near walls and even filling a large vug. The images in the middle and to the right show the pore system after forced drainage of water from Swi. Same colour code as first image.